Colloid Polym Sci 280:424–431 (2002)

ORIGINAL CONTRIBUTION

G.-S. Jang
W.-J. Cho
C.-S. Ha
W. Kim
H.-K. Kim

Morphology, crystallization behavior and properties of impact-modified polypropylene copolymer with or without sodium benzoate as a nucleating agent

Received: 4 June 2001
Accepted: 31 October 2001

G.-S. Jang · W.-J. Cho · C.-S. Ha (✉)
Department of Polymer Science
and Engineering
Pusan National University
Pusan 609–735, Korea
e-mail: csha@pnu.edu
Tel. +82-51-5102407
Fax: +82-51-514-4331

W. Kim
Department of Chemical Engineering
Pusan National University
Pusan 609–735, Korea

H.-K. Kim
Enbionet Co. Ltd.
Seoul 135–080, Korea

Present address: G.-S. Jang
LG-Caltex Oil Company
Technical Service Team
PP Working Group
Yosu 556–260, Korea

Abstract The morphology, crystallization behavior, and properties of an impact-modified polypropylene (PP) copolymer with or without sodium benzoate were investigated. The contents of ethylene–propylene rubber (EPR) in the reactor-made PP copolymer is about 15 wt%. For comparison, blends of PP and EPR containing the same EPR composition were prepared by melt-mixing. Morphological studies by scanning probe microscopy indicated that the impact-modified copolymer consists of three different phases, i.e., polyethylene, PP, and EPR phases, which is considerably different from the morphology of the conventional PP/EPR blend of the corresponding composition. The impact-modified PP copolymer exhibited a higher crystallization rate in terms of the lower crystallization half-time and thus higher thermal and mechanical properties, such as impact strength and hardness, than the PP/EPR blend did. The addition of sodium benzoate as a nucleating agent to the copolymer increased the crystallization rate and the mechanical properties.

Keywords Impact-modified polypropylene copolymer · Ethylene–propylene rubber · Crystallization behavior · Sodium benzoate

Introduction

Polypropylene (PP) has various excellent properties as a general-purpose resin, such as mechanical rigidity, thermal and chemical resistance, etc.; however, the poor impact strength at low temperature of PP limits its application in plastic industries [1–3]. One way to solve this problem is to add a rubber or polyethylene (PE) to PP. Ethylene–propylene rubber (EPR) has been used to improve the impact strength of PP. There are two ways of EPR addition to PP [4–7]. One is to blend EPR with PP [8–16]. The other is to prepare a reactor-made copolymer of PP and PE [11, 18–21]. Although a number of works has been published on the properties of PP/EPR blends, little is known about the structure and properties of the reactor-made PP copolymer.

The impact-modified PP copolymer in this work was prepared by in situ copolymerization of PP and EPR through two steps; propylene was polymerized to give PP, which was then copolymerized with EPR.

In this work, a PP/EPR blend was also prepared for comparison. The EPR composition in the blend was 15 wt%, corresponding to that in the in situ reactor-made impact-modified PP copolymer. Practically, 5–30 wt% of an elastomer such as EPR is blended with PP in order to sustain the balance of mechanical properties, such as impact strength and flexural modulus [2, 15]. It may be expected that the reactor-made impact-modified PP copolymer possess different morphology and properties from those of its corresponding PP/EPR blend.

We report here the morphology, crystallization behavior, and properties of the impact-modified PP copolymer in comparison with the PP/EPR blend. Sodium benzoate was used as a nucleating agent.

Experimental

Materials

Commercial grades of PP were supplied by LG-Caltex Oil Co. (Korea): M540 impact-modified copolymer and H540 homopolymer. M540 contains some fractions of EPR which had been obtained in another reactor by a cascade mode. It is characterized in terms of the weight percent of ethylene in the total polymer, E_t, the ethylene content in the rubber, E_c, and the rubber content in the total polymer, F_c. E_t, E_c, and F_c of M540 were determined to be 9.0, 60.5, and 14.9 wt%, respectively, by the supplier.

A commercial EPR copolymer, supplied by Kumho Polychem Co. (Korea), KEP-020P, was blended with PP (H540). The EPR possesses an ethylene content of 74 wt%, and a melt flow index of 3.2 g/10 min (at 230 °C, 2.16 kg). The PP/EPR blend with 15 wt% EPR was prepared in a 30-mm twin-screw extruder (MP2030, ATV, USA). Hereafter, the blend is designated as a "mechanical blend", whereas the reactor-made impact-modified PP copolymer is designated as an " in situ reactor blend", unless otherwise specified.

Sodium benzoate was supplied by the Fluid Energy Processing Equipment Co. (USA) and was used as a nucleating agent. The properties of materials used in this study are summarized in Table 1.

Specimens for the measurements of the mechanical properties were prepared using an injection-molding machine (IDE 75EN, Gold Star, Korea) at a melt temperature of 220 °C, a molding temperature of 50 °C, an injection time of 2 s, an injection pressure of 70 kgf/cm^2, a holding time of 13 s, a holdig pressure of 50 kgf/cm^2, and a cooling time of 30 s.

Methods

The dynamic mechanical properties were determined using a Rheometrics dynamic spectrometer (model RDS 2) using a specimen of 2-mm thickness. The heating rate was 5 °C/min in the temperature range from–100 to 40 °C, and the amplitude vibration was 0.2 mm.

The physical properties were measured according to ASTM test methods, such as D-790 for the flexural modulus and D-638 for the tensile strength, respectively, using a universal testing machine (6022, Instron, UK). The Gardener and Izod impact strengths were tested using the ASTM D-3029GC and D-256 methods, respectively. The heat distortion temperature was measured using the ASTM D-648 method.

The crystallization behavior was investigated using a PerkinElmer DSC-7 differential scanning calorimetry (DSC) calorimeter and a Leitz polarized optical microscope (POM; attached with a Mettler hot stage). In both the DSC and the POM analyses, the samples were heated to 200 °C and were kept at that temperature for 10 min to remove any thermal history before cooling them at a predetermined cooling rate (ranging from 1 to 20 °C/min) or to a predetermined crystallization temperature. The degree of crystallinity (X_c) was determined from the heat evolved during crystallization using the following equation:

$$X_c(\%) = \frac{\Delta H_c}{\Delta H_m^o} \times 100,$$

where ΔH_c is the heat of crystallization and $\Delta H_m{}^o$ is the heat of fusion for 100% crystalline PP (209 J/g for α-PP) [9, 15].

X-ray diffraction patterns were obtained with the Rigaku Denki X-ray diffractometer using nickel-filtered Cu Kα radiation (30 kV, 20 mA) in order to investigate the crystallization structure of the samples.

Scanning probe microscopy (SPM) (Thermomicroscopes, AutoProbe CP Research) was used to analyze the difference in the rubber morphology between the mechanical and the in situ reactor blend in this work. To obtain the SPM micrographs, injection-molded bars were used. The bar samples were primarily analyzed by pulsed-force microscopy; a specialized SPM imaging mode that allows stiffness, adhesion, and topography maps to be generated simultaneously. A small oscillation (frequency about

Table 1 Properties of materials. *MI*: melt flow index

Material	Properties	Value
M540	MI (g/10 min, 230 °C, 2.16 kg)	8
	Catalyst residue (wt ppm) Ti/Al/Cl	1.7/69/38
	Density (g/cm^3) solid/melt	0.903/0.734
	Molecular weight ($M_n/M_w/M_z \times 10^3$/Q)	98/330/959/3.4
	Ethylene content (wt%) $E_t/E_c/F_c$	9.0/60.5/14.9
H540	MI (g/10 min, 230 °C, 2.16 kg)	10
	Catalyst residue (wt ppm) Ti/Al/Cl	2.4/48/42
	Density (g/cm^3) solid/melt	0.903/0.734
	Molecular weight ($M_n/M_w/M_z \times 10^3$/Q)	108/360/1179/3.3
KEP-020P	MI (g/10 min, 230°C, 2.16 kg)	3.2
	Mooney viscosity (ML$_{1+4}$, 100 °C)	24
	Density (g/cm^3) solid	0.860
	C_3 content (wt%)	26
	T_g (°C)	–52
	Crystallinity (%)	3
Nucleating agent sodium benzoate	Formula	C_6H_5COONa
	Molecular weight	144.1
	Particle size (μm)	4
	Melting point (°C)	>300

380 Hz) was applied to the sample, which was periodically in contact with the cantilever. The deflection of the cantilever was monitored to produce curves that are similar to force–distance curves. For the intermittent contact images, the cantilever had a fairly high spring constant (about 40 N/m). The resonant frequency was near 300 kHz. The free amplitude was near 150 nm, while the set-point amplitude was near 110 nm, producing a ratio near 0.7. For pulsed-force imaging, the oscillation of the sample was near 380 Hz. The spring constant of the cantilever was near 1 N/m (contact cantilever). Phase imaging is useful for mapping a surface possessing materials with different mechanical properties, such as PP and EPR. In order to image the bulk material, the samples for analysis were carefully cryo-microtomed with glass knives at –120 °C.

Results and discussion

Morphology of impact-modified PP copolymer

The SPM micrographs of the impact-modified PP copolymer, M540, i.e., the “in situ reactor” blend, the M540 nucleated with sodium benzoate, M540N, and the PP/EPR (15%) blend (the “mechanical blend”) are shown in Fig. 1.

The morphology of the impact-modified PP copolymer resembles that of acrylonitrile–butadiene–styrene copolymer and shows the sea-island-within-sea-island structure [17]. The rubber (EPR) particles are easily identified in this micrograph as darker areas in the PP matrix. For the M540, lighter areas are also observed in the EPR regions. It may be suggested that this is largely due to the presence of a PE phase inside the EPR region. These lighter regions due to the presence of PE in the copolymer are observed in both M540 and M540N. Slight differences are observed between the lighter regions in the EPR domain for M540 and M540N. The size of the EPR domain was slightly smaller in case of M540N, which was nucleated with sodium benzoate.

The morphology of the mechanical blend, however, exhibits completely different morphology from that observed in the in situ reactor blend (M540 or M540N). The EPR domains are much smaller and are presented as streaks distributed in the PP matrix. No light regions appeared in the EPR domains as seen in the in situ reactor blend.

Nomura et al [14, 17] analyzed the three-dimensional morphology in comparison with the traditional sea-island structure. They reported that for a rubber-modified PP (i.e., ethylene–propylene block copolymer/EPR/talc blend system), blending of EPR with PP leads to an EPR phase, a PP phase and some mixed phases of EPR and PP. Some fraction mainly consisting of the PP phase in EPR can be dissolved in the atactic portion in PP. Then, the atactic (or amorphous) part of PP and EPR can form a network with each other and enhance the miscibility between the two components.

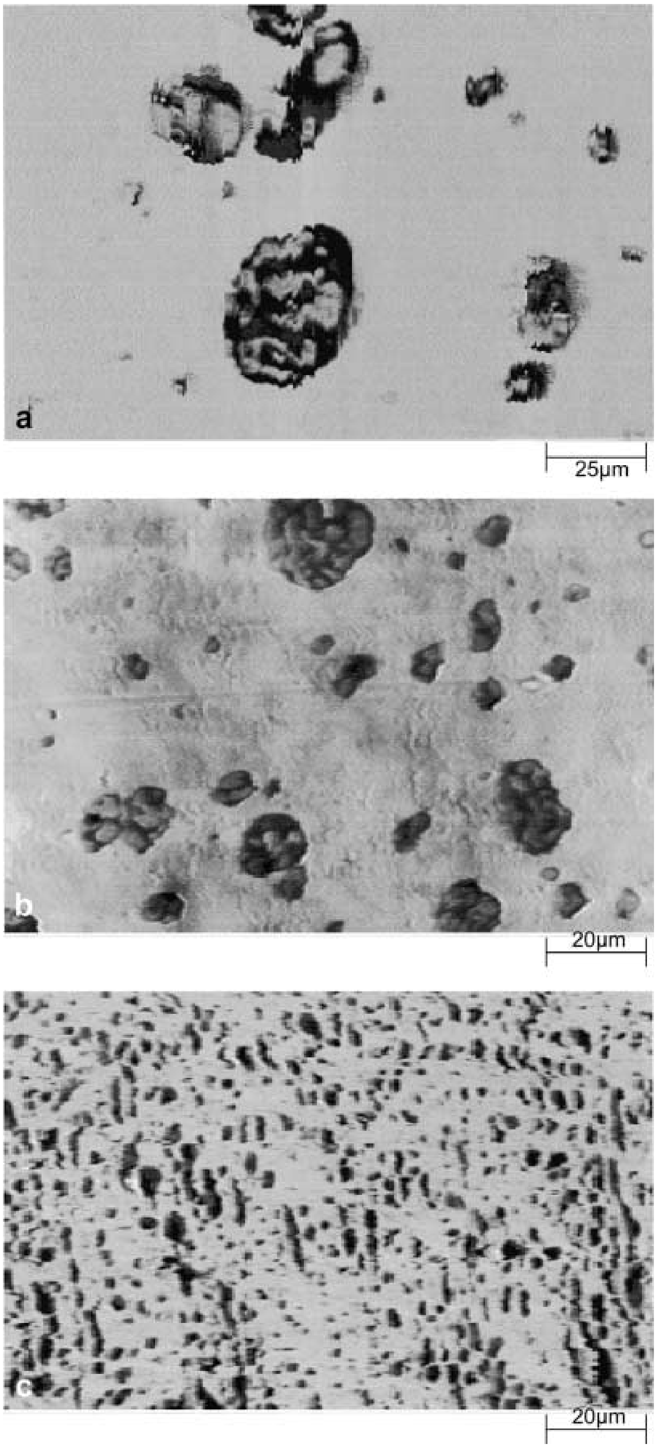

Fig. 1 Scanning probe micrographs (×75,000) of the in situ reactor blends with or without sodium benzoate and the mechanical blend: **a** M540, **b** M540N, *c* polypropylene (*PP*)/ethylene–propylene rubber (*EPR*) (15 wt%)

Figure 2 shows that there are slight differences in the crystallization thermograms: the in situ reactor blend (M540) has two crystallization peaks of PP (113.6 °C)

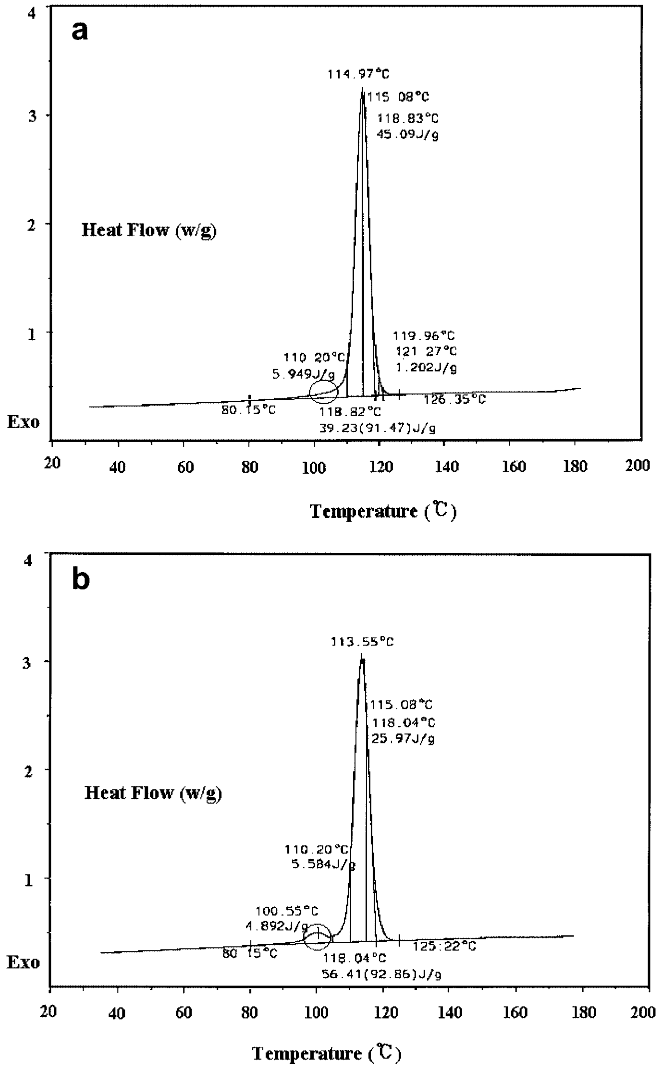

Fig. 2 Differential scanning calorimetry thermograms of melting crystallization at a cooling rate of 10 °C/min: **a** mechanical blend, **b** in situ reactor blend, M540

and PE (100.6 °C), while the mechanical blend exhibits a single crystallization peak (115.0 °C). The result suggests that the in situ reactor blend, i.e., the M540 copolymer, possesses a PE phase as well as a PP phase.

Similarly, Ito et al. [19] reported the annealing of a block PP, which was a commercial product of Tokyuma Soda of Japan and which was prepared by manner similar to that of the impact-modified PP copolymer used in this work. They showed that there are three endothermic peaks on the DSC thermograms for the sample extracted by *n*-heptane, indicating that they are attributed to the PE phase near 120 °C, the PP phase at about 150 °C, and partial fusion of crystalline EPR below 120 °C, respectively.

When they crystallize in the melt phase, such complicated phenomena as diffusion by crystallization and diffusion at each phase interface accompany each other: crystalline EPR undergoes crystallization at the interface with the PP matrix or the PE domain, resulting in an increase in miscibility at the interface and a thickening of the segmental interface layer. The crystallization of the PP matrix is followed by migration of atactic PP and high-molecular-weight amorphous EPR from the crystalline region to the amorphous region (spherulite interface or EPR domain).

Crystallization behavior

The isothermally polarized micrographs for the in situ reactor blend and the mechanical blend at the isothermal crystallization temperature of 138 °C are shown in Fig. 3. A substantial difference was observed in the micorgraphs, i.e., in the case of the in situ reactor blend, the spherulites are very small and dense, and the spherulitic growth rate is very high, whereas for the

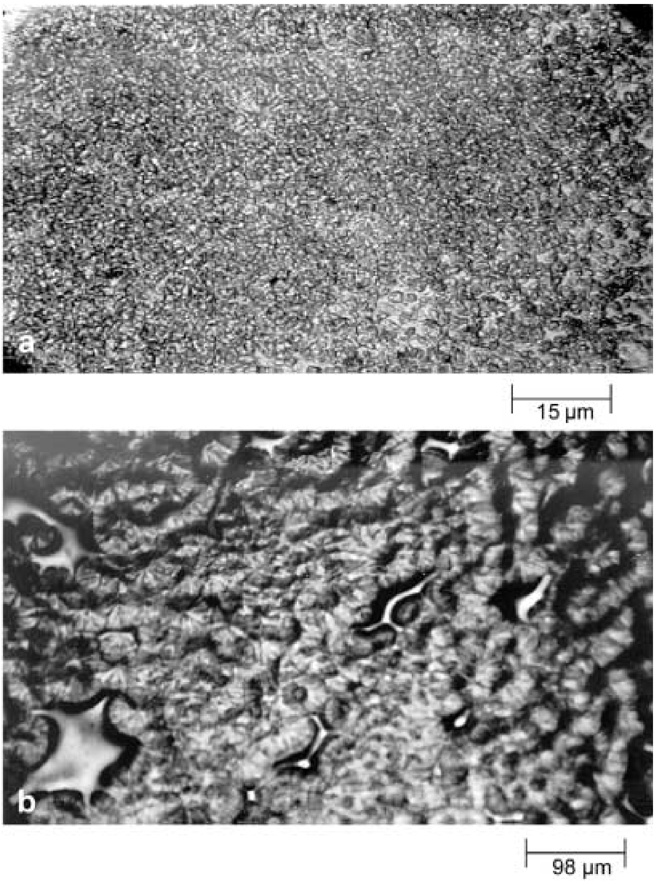

Fig. 3 Polarized micrographs (×100) of the in situ reactor blend and the mechanical blend at the crystallization temperature of 138 °C: **a** M540, **b** PP/EPR (15 wt%)

Table 2 Comparision of crystallization properties of the mechanical blend and the in situ reactor blends. The cooling rate is 10 °C/min. Polypropylene (*PP*), ethylene–propylene rubber (*EPR*)

Blend	Sample	ΔH_m (J/g)	T_c (°C)	X_c (%)
Mechanical	PP/EPR (15 wt%)	70.5	115.0	43.8
In situ reactor	M540	104.2	113.6	44.4
In situ reactor	M540N	105.1	124.9	45.7

mechanical blend, the spherulites are large and thin, and the spherulite growth rate is very low.

The crystallization properties of the mechanical blend and the in situ reactor blend with or without sodium benzoate are compared in Table 2. The crystallization temperature data show that M540N has a higher crystallization temperature, T_c, than M540 owing to the nucleation effect of sodium benzoate, but M540 has a T_c value similar to the mechanical blend. In case of crystallinity (X_c), M540N shows a higher value than the mechanical blend and is slightly higher than M540. The higher heat of fusion, ΔH_m, values of both M540 and M540N in comparison to the mechanical blend may be due to the presence of the PE phase in the in situ reactor blends.

In order to investigate the crystallization rate for nonisothermal crystallization, the crystallization rate parameter (CRP) was estimated from the slope of the plot of the inverse of the crystallization half-time versus the cooling rate according to the method proposed by Zhang et al. [22]. The higher the cooling rate, the higher the supercooling of crystallization, the faster the nucleation. The faster the crystallization of a polymer, the greater the slope.

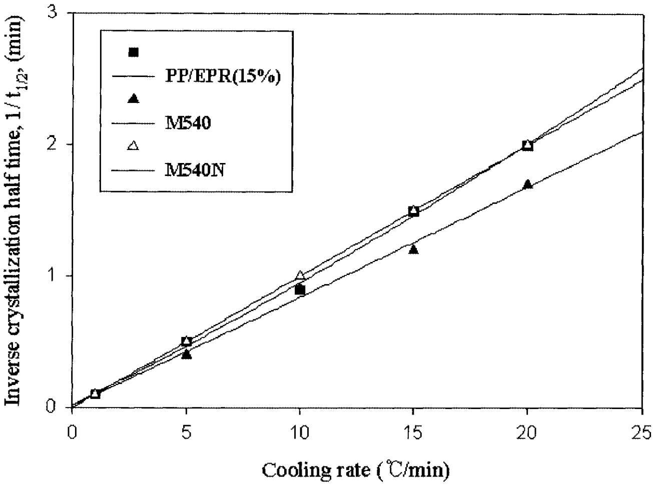

Fig. 4 Inverse crystallization half-time versus cooling rate of the in situ reactor blends with or without sodium benzoate and the mechanical blend. The crystallization rate parameter was determined from the slope of this plot

As shown in Fig. 4, we can find the change in the CRP values for the samples. The result suggests that the crystallization rate of M540N is slightly higher than or almost equal to that of the mechanical blend, but it is much higher than that of M540 owing to the nucleating effect of the sodium benzoate. Details of the nucleation effect of sodium benzoate in the crystallization of PP are described elsewhere [23].

In the case of a binary blend, if the second polymer dispersed in a crystallizable matrix crystallizes under similar conditions as the matrix polymer, crystals of the second polymer can grow at interfaces [24] and may act as a nucleating agent for the crystallization of the matrix [25–30]. Such behavior may be found both in the mechanical blend and in the situ reactor blend as in the PP/high-density PE blend. It should be noted, however, that the EPR shows a different degree of crystallinity depending on the C2/C3 ratios, i.e., a solid PP-phase-like crystallinity predominates for higher C3 contents and a PE-phase-like crystallinity predominates for higher C2 contents [31–33].

The trace of PE of EPR in our blends was observed by DSC, as shown in Fig. 2. For comparison, the crystallization data of high-density PE (2200J: Honam Petrochemical Co., Korea) is presented in Table 3.

A little PE sourced from EPR of the blends crystallizes below 125 °C with a rate close to that of the crystallization of PP. Fast nonisothermal crystallization can also take place according to a simultaneous crystallization of both components. Already-crystallized inclusions of a dispersed polymer accelerate the crystallization of a matrix, acting as a nucleating agent, and induce the formation of additional spherulites [28, 29, 30, 34]. Finally, the average spherulite radius in the blend becomes smaller than in the unnucleated PP crystallized under same conditions. Such speculations can be indirectly proven if Figs. 3 and 4 are considered.

In the PP/EPR blend, major factors influencing the crystallization behavior may be a combination of not only impurities including sodium benzoate as a nucleating agent for PP but also PE sourced from EPR in the blend. In fact, the latter compared to the former will not be as large as expected because of the low high-density PE content generated by the C2-rich composition in the mechanical blend.

Table 3 Crystallization properties of EPR and high-density polyethylene (*HDPE*) (at a cooling and heating rate of 10 °C/min)

	ΔH_m (J/g)	T_m (°C)	T_c (°C)	X_c (%)	ΔH_c (J/g)
EPR (KEP-020P)	1.4	42.6	11.5	4.0[a]	9.0
HDPE (2200 J)	211.4	131.2	114.2	79.4[b]	231.3

[a] H_c^o=209 J/g
[b] H_c^o=291.3 J/g

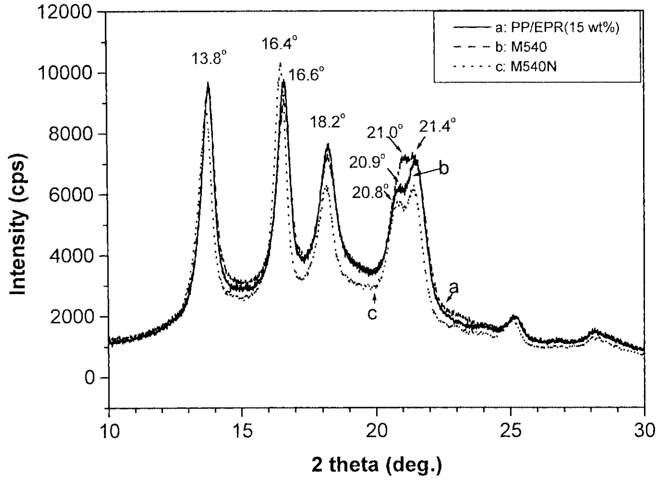

Fig. 5 X-ray diffractograms of the in situ reactor blends with or without sodium benzoate and the mechanical blend: *a* PP/EPR (15 wt%), *b* M540, *c* M540N

The X-ray diffractions of the PP/EPR blend, M540, and M540N are shown in Fig. 5. The X-ray diffractions of all the samples showed four sharp crystalline reflection peaks, in the region of the Bragg angle (2θ) between 10° and 50°. Those strong diffraction peaks are located at the diffraction angles 2θ around 13.8°, 16.6°, 18.2°, and 21.4° (doublet), of which the first three peaks correspond to the (110), (040), and (130) planes, respectively, and are characteristic of the typical α-form monoclinic structure of PP [35]. Careful inspection of Fig. 5 indicates, however, that in the case of M540N the diffraction maximum of the PP crystal at $2\theta = 16.6°$ shifted to a lower angle (16.4°) and its intensity decreased, and the relative diffraction maximum at $2\theta = 20.8–21.4°$ increased in comparison to those of the PP/EPR blend and M540, whereas the intensities of the diffraction maxima at $2\theta = 13.8°$ and 18.2° decreased. This result means that some traces of the β-form and/or the γ-form crystalline structures of PP exist in M540N [35, 36]. The slight alteration of the crystalline structure of PP by sodium benzoate for M540N may come from the complex morphology of the M540 containing PE and EPR phases, although the exact mechanism is not clear at the moment.

Dynamic mechanical properties

The dynamic mechanical analyzer (DMA) spectra of the blends show that there are three transition points in the plot of the loss modulus, G'', as a function of temperature, i.e., the first at about 5 °C, the second from −52 to −57 °C, and the third in the vicinity below −80 °C (Fig. 6). It may be thought that the three transitions indicate the existence of three phases in the blends, suggesting the glass-transition temperatures of the PP, EPR, and PE phases, respectively [3, 4, 5, 8, 17, 19, 35, 37]. As shown in Table 4, M540N shows slightly higher glass-transition temperatures for the PP phase and the

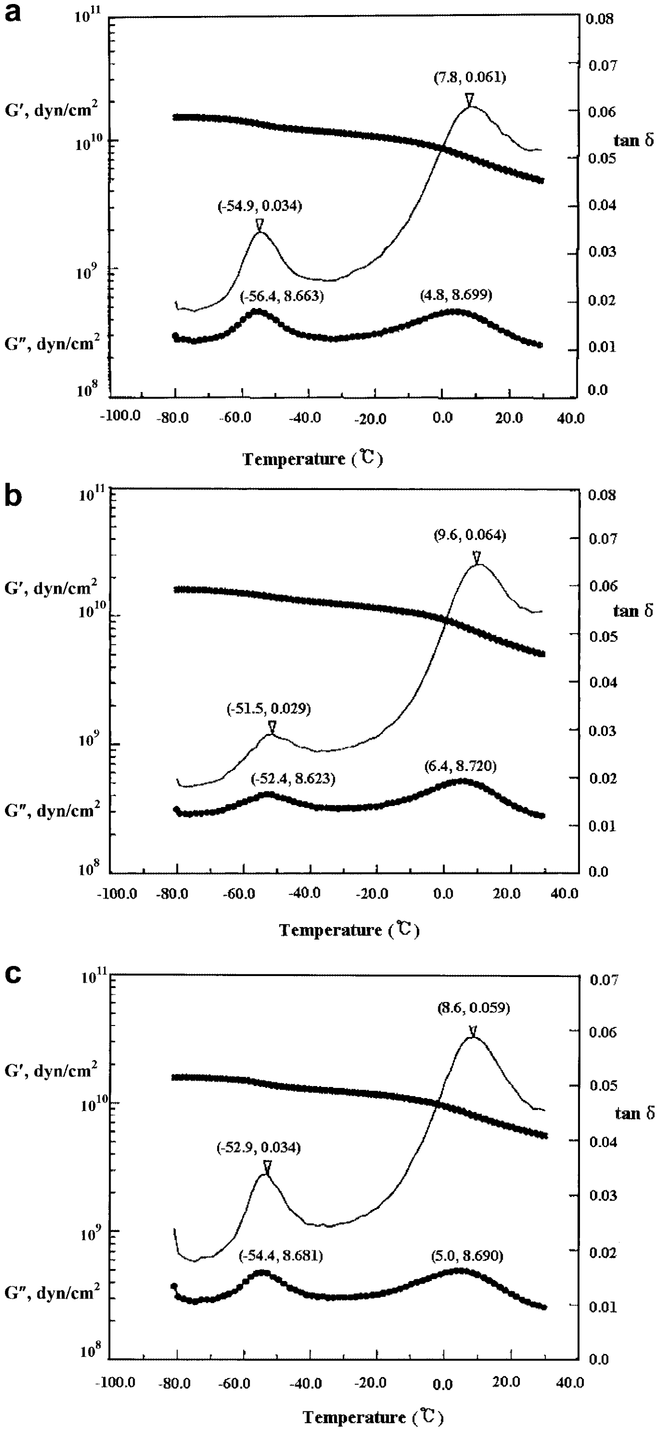

Fig. 6 Dynamic mechanical properties of the in situ reactor blends with or without sodium benzoate and the mechanical blend: **a** M540, **b** PP/EPR (15 wt%), **c** M540N

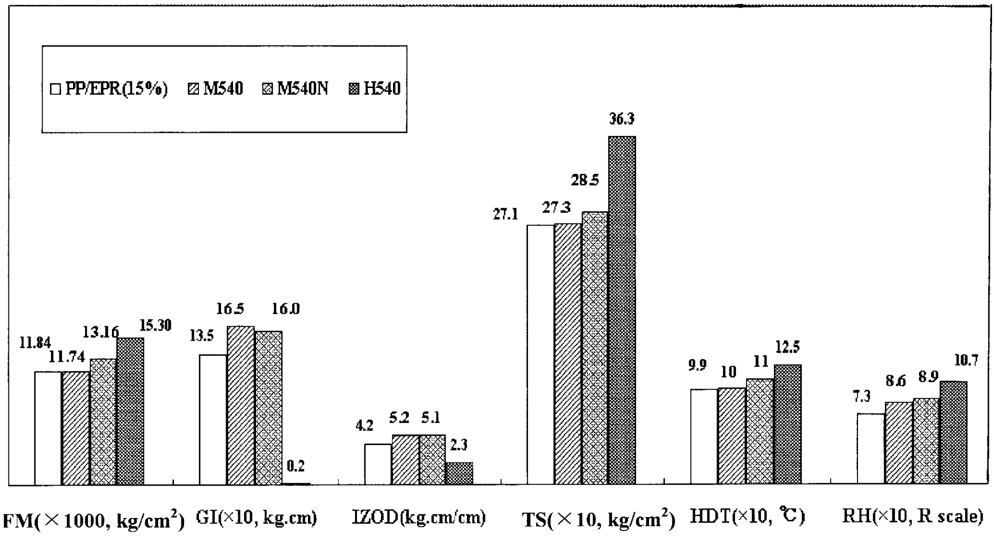

Fig. 7 Mechanical properties of the in situ reactor blends with or without sodium benzoate, the mechanical blend, and H540. Flexural modulus (*FM*), Gardener impact strength(*GI*), Izod impact strength (*IZOD*), tensile strength (*TS*), heat distortion temperature (*HDT*), Rockwell hardness (*RH*)

Table 4 Comparision of dynamic mechanical properties of the mechanical blend and the in situ reactor blends. $\tan\delta = G''/G'$

		PP/EPR (15 wt%)	M540	M540N
PP phase	T_g (°C)	6.4	4.8	5.0
	G'' (dyne/cm^2)	8.720	8.699	8.690
EPR phase	T_g (°C)	–52.4	–56.4	–54.4
	G'' (dyne/cm^2)	8.623	8.663	8.681

EPR phase than M540 owing to the nucleating effect of sodium benzoate, though the difference is not large. Also, there was no significant difference in the absolute values of the storage modulus, G', and G'' for all the blends.

Mechanical properties

The mechanical properties of the mechanical and the in situ reactor blend as well as H540 are shown in Fig. 7. It should be noted that M540N generally shows greater mechanical properties, such as tensile strength, heat distortion temperature, and Rockwell hardness, etc. as well as impact strength, than the mechanical blend. The result may be due to the presence of PE in the in situ reactor blend, whereas there is no PE phase in the mechanical blend. In addition, the nucleated M540N generally exhibits greater mechanical properties than the unnucleated blend, M540, owing to the nucleating effect of sodium benzoate. It should be noted that both the in situ reactor blends and the mechanical blend show significantly enhanced impact strength compared to the PP homopolymer, H540, owing to the presence of 15 wt% of EPR, even though their mechanical properties are generally low in comparison to H540.

Conclusions

By DSC, SPM, and DMA analyses, the in situ reactor blend, M540 copolymer, was confirmed to consist of multiple phases: PP, EPR (crystalline and amorphous), and PE. Especially, the SPM investigations showed that there is a considerable difference between the morphology of the mechanical and the in situ reactor blends. M540 had a significant effect on the crystallization properties and the dynamic/physical properties of the copolymer as well as of the PP/EPR blend.

When they crystallize in the melt phase, it may be assumed that a complicated phenomenon including diffusion by crystallization and diffusion at each phase interface might occur simultaneously and competitively. As a result, the crystallization behavior, effecting compatibilization at the interface, lowering the glass-transition temperature of the system, causes the increase in the interfacial bonding strength to improve the impact strength, etc. Crystallizations of these types are further accelerated by sodium benzoate used as a nucleating agent.

It was found that M540 as well as M540N generally show greater mechanical properties, such as tensile strength, heat distortion temperature, Rockwell hardness, etc., than the mechanical blend, owing to the presence of PE in the in situ reactor blends, whereas there is no PE phase in the mechanical blend.

Acknowledgements The authors express appreciation to not only S.R. Woo, and Y.M. Jang of LG-Caltex Co. for providing much time for preparing this article but also to Bill Sheard and Les Manner of the UCC Technical Center for obtaining the SPM micrographs. The work was supported by the Center for Integrated Molecular Systems, POSTECH, Korea, and the Brain Korea 21 Project in 2001. W.K. thanks the Institute of Environmental Technology and Industry, Pusan National University, Korea (99-10-05-03-A-3).

References

1. Walsh DJ, Higgins JS, Macconachie A (1985) Polymer blends and mixtures. Imperial College, London, pp 457–463
2. Tjong SC, Xu SA (1997) Polym Int 44: 95
3. Ito J, Mitani K, Mizutani Y (1992) J Appl Polym Sci 46:1221
4. Moore EP (1996) Polypropylene handbook. Hanser, New York, pp 149–164
5. Union Carbide Corporytion (1986) Technical manual, vol IV. Product technology. Union Carbide Corporation, Danbury
6. Nomura T, Nishio T, Sato H, Sano H (1993) Kobunshi Ronbunshu 50:27
7. Nomura T, Nishio T, Moriya S, Hashimoto M (1994) Kobunshi Ronbunshu 51:569
8. Karger-Kocsis J, Kiss L (1987) Polym Eng Sci 27:254
9. Dorazio L, Mancarella C, Martuscelli E, Sticotti G (1991) J Mater Sci 26:4033
10. Yokoyama Y, Ricco T (1997) J Appl Polym Sci 66:1007
11. Dorazio L, Mancarella C, Martuscelli E, Sticotti G (1993) Polymer 34:3671
12. Debling JA, Zacca JA, Ray WH (1997) Chem Eng Sci 52:111
13. Tribout C, Monasse B, Haudin JM (1996) Colloid Polym Sci 274:197
14. Nomura T, Nishio T, Sato H, Sano H (1993) Kobunshi Ronbunshu 50:19
15. Avalos F, Lopez-Manchado MA, Arroyo M (1996) Polymer 37:5681
16. Ha CS, Kim SC (1989) J Appl Polym Sci 37:317
17. Nomura T, Nishio T, Sato H, Sano H (1993) Kobunshi Ronbunshu 50:87
18. Nitta K, Kawada T, Yamahiro M, Mori H, Terano M (2000) Polymer 41:6765
19. Ito J, Mitani K, Mizutani Y (1992) J Appl Polym Sci 46:1235
20. Walsh DJ, Higgins JS, Macconachie A (1985) Polymer blends and mixtures. Imperial College, London, p 219
21. Fumio I (1998) Practical polymer alloy design. Industrial Investigation, Tokyo, pp 119–135
22. Zhang R, Zheng H, Lou X, Ma D (1994) J Appl Polym Sci 1:51
23. Jang GS, Cho WJ, Ha CS (2001) J Polym Sci Part B Polym Phys 39:1001
24. Duvall J, Sllitti C, Myers C, Hiltner A, Baer E (1994) J Appl Polym Sci 52: 207
25. Lustiger A, Marzinsky CN, Mueller RR (1998) J Appl Polym Sci Part B 36:2047
26. Varga J, Karger-Kocsis J (1995) Polym Commun 36:4877
27. Bartczak Z, Galeski A, Pracella M (1986) Polymer 27:537
28. Siegmann A (1979) J Appl Polym Sci 24:2333
29. Teh JW (1983) J Appl Polym Sci 28:605
30. Lovinger A, Williams ML (1980) J Appl Polym Sci 25:1703
31. Greco R, Mancarella C, Martuscelli E (1987) Polymer 28:1929
32. Greco R, Martuscelli E, Ragosta G, Yin J (1988) J Mater Sci 23:307
33. Ananda MC (1998), ANTEC '98 2:1875
34. Fench H, Jungnickel BJ (1989) Colloid Polym Sci 267:16
35. Ha CS, Kim SC (1988) J Appl Polym Sci 35:2211
36. van der Ven S (1990) Polypropylene and other Polyolefins. Elsevier, Amsterdam, p 198
37. Fumio I (1998) Practical polymer alloy design. Industrial Investigation, Tokyo, pp 219–237